PERGAMON

International Journal of Engineering Science 40 (2002) 51–66

International Journal of Engineering Science

www.elsevier.com/locate/ijengsci

Wiener–Hopf analysis of the two-dimensional box-like horn radiator

Filiz Birbir, Alinur Büyükaksoy *, Vitaliy P. Chumachenko [1]

Department of Mathematics, Gebze Institute of Technology, P.O. Box 141, Gebze, Kocaeli, Turkey

Received 12 January 2001; received in revised form 26 January 2001; accepted 7 March 2001

(Communicated by H. DEMIRAY)

Abstract

A hybrid method consisting of employing the mode-matching method in conjunction with the Fourier transform technique is used to analyze the radiation of the dominant TEM-wave from a two-dimensional rectangular horn. The hybrid method that we will adopt reduces the related boundary value problem into a scalar modified Wiener–Hopf equation of the third kind. The solution involves branch-cut integrals which are evaluated approximately and infinitely many unknown constants satisfying an infinite system of linear algebraic equations susceptible to a numerical treatment. Some computational results illustrating the effects of various parameters such as waveguide width, horn length, etc., on the radiation phenomenon are also presented. Comparison of the results with those obtained for a similar finite structure is proved satisfactory.

1. Introduction

As is well known, different types of electromagnetic horns are commonly used as primary feeds in reflector antenna systems used in microwave communication. These horns are obtained, in general, by flaring out waveguides of different cross-sections. To analyze the performance of the system, one needs to know accurately the near- and far-field patterns of horns. To this end, different analytical and/or numerical techniques are developed. For example, an E-plane radiation pattern was studied by Yu et al. [1] by considering multiply reflected images. Yu and Rudduck [2] obtained the H-plane pattern using the geometrical theory of diffraction (GTD) and parallel plate

* Corresponding author.

E-mail address: alinur@penta.gyte.edu.tr (A. Büyükaksoy).

[1] On leave of absence from Technical University of Zaporizhzhya, 64 Zhukovsky Str., Zaporizhzhya, 330063, Ukraine.

PII: S0020-7225(01)00053-2

waveguide mode approximation. This was refined by Mentzer et al. [3] and by Narasiman and Rao [4] using the uniform theory of diffraction (UTD) slope diffraction correction. The near-and far-field E- and H-plane patterns were found in [4] using a spherical source excitation. A uniform asymptotic theory (UAT) has been used by Menendez and Lee [5] on rectangular horns considering up to $k^{-1/2}$ terms and rectangular waveguide modes were approximated by parallel plates waveguide modes. A different approach for analyzing two-dimensional horns is provided by P'yankov and Chumachenko [6] and P'yankov [7] who used a method of solution based on expansion in terms of Mathieu functions related to linear chains of boundary forming the horn.

In the present work the radiation of the dominant TEM mode from a two-dimensional box-like horn, formed by flaring out a parallel plate waveguide (see Fig. 1), is rigorously analyzed through the Wiener–Hopf technique. The advantage of the Wiener–Hopf technique over the other methods is that it is rigorous in the sense that the edge condition is explicitly incorporated into the analysis and that it provides accurate and reliable results over a broad frequency range. This method can also easily be generalized to the case where the walls of the horn are impedance boundaries. Furthermore, contrary to the numerical techniques which are efficient only for boundaries of limited length, the Wiener–Hopf method does not require such a restriction.

In what follows, a hybrid method of formulation which consists of employing Fourier transform technique in conjunction with a mode-matching method will be adopted [8,9]. By expanding the diffracted field into a series of normal modes in the waveguide region and using the Fourier transform technique elsewhere, we get a scalar modified Wiener–Hopf equation of the third kind. The solution of the Wiener–Hopf equation contains branch-cut integrals involving unknown integrands and a set of infinitely many constants satisfying an infinite system of linear algebraic equations. The branch-cut integrals are evaluated asymptotically and a numerical solution of the set of linear algebraic equations is obtained for various values of the waveguide width, the step height and the horn length, wherefrom the effect of these parameters on the diffraction phenomenon is studied. It is shown that the above results agree well with the ones obtained for a similar finite structure by applying the method described in [6,7].

A time factor $e^{-i\omega t}$ is assumed and suppressed throughout the paper.

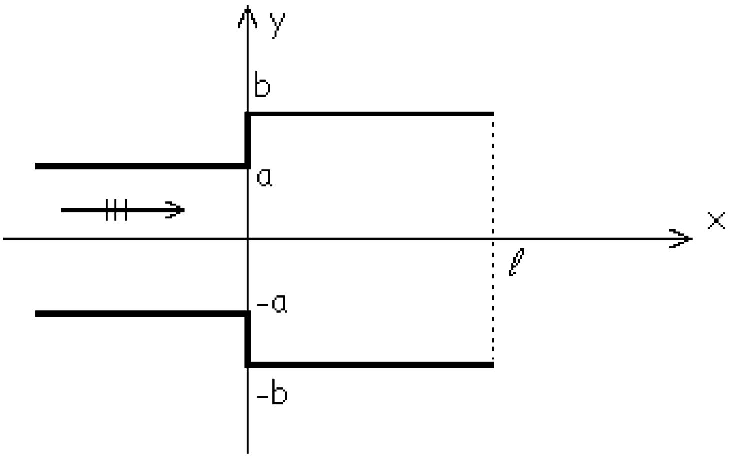

Fig. 1. Two-dimensional box-like horn radiator.

2. Formulation and solution of the problem

2.1. Formulation of the problem

We consider the radiation of the dominant TEM mode from the two-dimensional box-like horn radiator shown in Fig. 1. Due to the symmetry of the structure and the excitation, the problem in Fig. 1 is reduced to the equivalent one depicted in Fig. 2, where an infinite perfectly conducting plate (electric wall) is placed at $y = 0$. In the equivalent problem, the dominant TEM mode is incident from the left in the parallel plate region formed by the infinite plane $S_1 = \{x \in (-\infty, \infty),\ y = 0,\ z \in (-\infty, \infty)\}$ and the parallel plates $S_2 = \{x \in (-\infty, 0),\ y = a,\ z \in (-\infty, \infty)\}$ and $S_3 = \{x \in (0, \ell),\ y = b,\ z \in (-\infty, \infty)\}$ joined together by a step defined by $S_4 = \{x = 0,\ y \in (a, b),\ z \in (-\infty, \infty)\}$ (Fig. 2). Notice that all the plates are assumed to be perfectly conducting.

The configuration is two-dimensional and with the assumed incident field, only three field components, namely:

$$H_z = u(x,y), \quad E_x = \frac{\mathrm{i}}{\omega\varepsilon_0}\frac{\partial}{\partial y}u(x,y) \quad \text{and} \quad E_y = -\frac{\mathrm{i}}{\omega\varepsilon_0}\frac{\partial}{\partial x}u(x,y)$$

are nonzero.

For analysis purposes, it is convenient to express the total field as follows:

$$u(x,y) = \begin{cases} u_1(x,y), & y > b, \quad x \in (-\infty, \infty), \\ u_2(x,y), & y \in (a,b), \quad x < 0, \\ u_3(x,y) + u^{\mathrm{i}}(x,y), & y \in (0,a), \quad x < 0, \\ u_4(x,y), & y \in (0,b), \quad x \in (0,\ell), \\ u_5(x,y), & y \in (0,b), \quad x > \ell. \end{cases} \tag{1a}$$

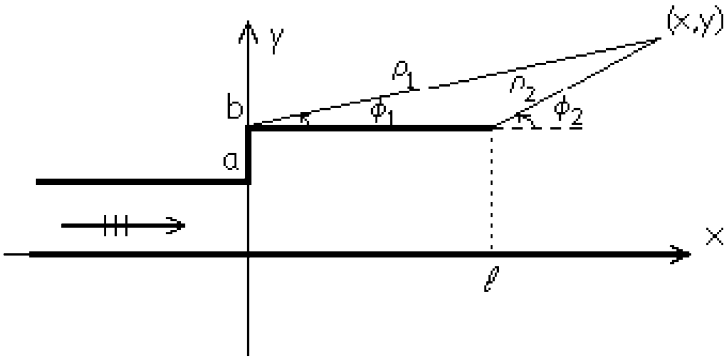

Fig. 2. Equivalent problem for incident dominant TEM mode.

Here, u^{i} is the incident field given by

$$u^{\mathrm{i}}(x,y) = \mathrm{e}^{\mathrm{i}kx} \tag{1b}$$

with k being the wave number of the space which is supposed to be dissipative with a very small $\Im m(k) > 0$. At the end of the analysis we will make $\Im m(k) \to +0$.

The total field $u(x,y)$, which satisfies the Helmholtz equation,

$$\left(\frac{\partial^2}{\partial x^2} + \frac{\partial^2}{\partial y^2} + k^2\right)u(x,y) = 0, \tag{2}$$

is to be determined with the aid of the following boundary and continuity conditions:

$$\frac{\partial}{\partial y}u_1(x,b) = 0, \quad x \in (0,\ell), \tag{3a}$$

$$\frac{\partial}{\partial x}u_2(0,y) = 0, \quad y \in (a,b), \tag{3b}$$

$$\frac{\partial}{\partial y}u_2(x,a) = 0, \quad x \in (-\infty,0), \tag{3c}$$

$$\frac{\partial}{\partial y}u_3(x,0) = 0, \quad x \in (-\infty,0), \tag{3d}$$

$$\frac{\partial}{\partial y}u_4(x,0) = 0, \quad x \in (0,\ell), \tag{3e}$$

$$\frac{\partial}{\partial y}u_5(x,0) = 0, \quad x \in (0,\infty), \tag{3f}$$

$$u_1(x,b) = u_2(x,b), \quad x < 0, \tag{3g}$$

$$\frac{\partial}{\partial y}u_1(x,b) = \frac{\partial}{\partial y}u_2(x,b), \quad x < 0, \tag{3h}$$

$$u_1(x,b) = u_5(x,b), \quad x > \ell, \tag{3i}$$

$$\frac{\partial}{\partial y}u_1(x,b) = \frac{\partial}{\partial y}u_5(x,b), \quad x > \ell, \tag{3j}$$

$$u_3(0,y) + 1 = u_4(0,y), \quad y \in (0,a), \tag{3k}$$

$$\frac{\partial}{\partial x}u_3(0,y) + \mathrm{i}k = \frac{\partial}{\partial x}u_4(0,y), \quad y \in (0,a), \tag{3l}$$

$$u_4(0,y) = u_5(0,y), \quad y \in (0,b), \tag{3m}$$

$$\frac{\partial}{\partial x}u_4(0,y) = \frac{\partial}{\partial x}u_5(0,y), \quad y \in (0,b). \tag{3n}$$

2.2. Reduction to modified Wiener–Hopf equations

Since $u_1(x,y)$ satisfies the Helmholtz equation in the range $x \in (-\infty,\infty)$, its Fourier transform with respect to x, namely,

$$F(\alpha,y) = \int_{-\infty}^{\infty} u_1(x,y)\mathrm{e}^{\mathrm{i}\alpha x}\,\mathrm{d}x, \tag{4a}$$

satisfies

$$\left[\frac{\mathrm{d}^2}{\mathrm{d}y^2} + \left(k^2-\alpha^2\right)\right]F(\alpha,y) = 0. \tag{4b}$$

It is convenient to split the function $F(\alpha,y)$ into a sum of three parts as follows:

$$F(\alpha,y) = F_-(\alpha,y) + F_1(\alpha,y) + \mathrm{e}^{\mathrm{i}\alpha\ell}F_+(\alpha,y), \tag{4c}$$

where

$$F_-(\alpha,y) = \int_{-\infty}^{0} u_1(x,y)\mathrm{e}^{\mathrm{i}\alpha x}\,\mathrm{d}x, \tag{4d}$$

$$F_1(\alpha,y) = \int_{0}^{\ell} u_1(x,y)\mathrm{e}^{\mathrm{i}\alpha x}\,\mathrm{d}x, \tag{4e}$$

and

$$F_+(\alpha,y) = \int_{\ell}^{\infty} u_1(x,y)\mathrm{e}^{\mathrm{i}\alpha(x-\ell)}\,\mathrm{d}x. \tag{4f}$$

By taking into account the obvious asymptotic behaviors of u_1 for $x \to \pm\infty$, namely,

$$u_1(x,y) = \mathrm{O}\left(\mathrm{e}^{\mathrm{i}k|x|}\right), \quad \text{as } x \to \pm\infty, \tag{5}$$

one can show that $F_+(\alpha,y)$ and $F_-(\alpha,y)$ are regular functions of α in the half-planes $\Im m(\alpha) > \Im m(-k)$ and $\Im m(\alpha) < \Im m(k)$, respectively, while $F_1(\alpha,y)$ is an entire function. The general solution of (4b) satisfying the radiation condition for $y \to \infty$ reads

$$F_-(\alpha,y) + F_1(\alpha,y) + \mathrm{e}^{\mathrm{i}\alpha\ell}F_+(\alpha,y) = A(\alpha)\mathrm{e}^{\mathrm{i}K(\alpha)(y-b)}, \tag{6}$$

where $K(\alpha)$ denotes the square root function $K(\alpha) = \sqrt{k^2-\alpha^2}$ defined in the complex α-plane cut from $\alpha = k$ to $\alpha = k\infty$ and $\alpha = -k$ to $\alpha = -k\infty$ such that $K(0) = k$.

In terms of the Fourier transform domain, (3a) takes the following form:

$$\dot{F}_1(\alpha,b) = 0, \tag{7}$$

where the dot on $\dot{F}_1$ refers to specify the derivative with respect to y. By using the derivative of (6), with respect to y, in (7), we get

$$\dot{F}_-(\alpha, b) + e^{i\alpha\ell}\dot{F}_+(\alpha, b) = iK(\alpha)A(\alpha). \tag{8}$$

Eq. (2) is also satisfied in the region $\{a < y < b,\ x < 0\}$ by $u_2(x, y)$ and in the region $\{0 < y < b,\ x > \ell\}$ by $u_5(x, y)$, which yields

$$\left[\frac{d^2}{dy^2} + K^2(\alpha)\right]G_-(\alpha, y) = i\alpha f(y) \tag{9a}$$

and

$$\left[\frac{d^2}{dy^2} + K^2(\alpha)\right]G_+(\alpha, y) = g(y) - i\alpha h(y), \tag{9b}$$

where

$$G_-(\alpha, y) = \int_{-\infty}^{0} u_2(x, y)e^{i\alpha x}\,dx, \tag{10a}$$

$$G_+(\alpha, y) = \int_{\ell}^{\infty} u_5(x, y)e^{i\alpha(x-\ell)}\,dx, \tag{10b}$$

and

$$f(y) = u_2(0, y), \tag{10c}$$

$$g(y) = \frac{\partial}{\partial x}u_5(\ell, y), \tag{10d}$$

$$h(y) = u_5(\ell, y), \tag{10e}$$

Eq. (3a) being taken into account. Notice that $G_-(\alpha, y)$ and $G_+(\alpha, y)$ are regular in the half-planes $\Im m(\alpha) < \Im m(k)$ and $\Im m(\alpha) > \Im m(-k)$, respectively.

The general solutions of (9a) and (9b) satisfying (3c) at $y = a$ and (3f) at $y = 0$ read:

$$G_-(\alpha, y) = D_1(\alpha)\cos K(y - a) + \frac{i\alpha}{K}\int_a^y f(t)\sin K(y - t)\,dt, \tag{11a}$$

$$G_+(\alpha, y) = D_2(\alpha)\cos Ky + \frac{1}{K}\int_0^y [g(t) - i\alpha h(t)]\sin K(y - t)\,dt. \tag{11b}$$

Here, $D_1(\alpha)$ and $D_2(\alpha)$ stand for two yet unknown integration constants. Using (3h) and (3j), these latter can be solved uniquely as follows:

$$D_1(\alpha) = -\frac{1}{K\sin K(b - a)}\left\{\dot{F}_-(\alpha, b) - i\alpha\int_a^b f(t)\cos K(b - t)\,dt\right\} \tag{12a}$$

and

$$D_2(\alpha) = -\frac{1}{K\sin Kb}\left\{\dot{F}_+(\alpha,b) - \int_0^b [g(t) - \mathrm{i}\alpha h(t)]\cos K(b-t)\,\mathrm{d}t\right\}. \tag{12b}$$

Substituting (12a) into (11a) and (12b) into (11b) we get

$$\begin{aligned} G_-(\alpha,y) = &-\frac{\cos K(y-a)}{K\sin K(b-a)}\left\{\dot{F}_-(\alpha,b) - \mathrm{i}\alpha\int_a^b f(t)\cos K(b-t)\,\mathrm{d}t\right\} \\ &+\frac{\mathrm{i}\alpha}{K}\int_a^y f(t)\sin K(y-t)\,\mathrm{d}t \end{aligned} \tag{13a}$$

and

$$\begin{aligned} G_+(\alpha,y) = &-\frac{\cos Ky}{K\sin Kb}\left\{\dot{F}_+(\alpha,b) - \int_0^b [g(t) - \mathrm{i}\alpha h(t)]\cos K(b-t)\,\mathrm{d}t\right\} \\ &+\frac{1}{K}\int_0^y [g(t) - \alpha h(t)]\sin K(y-t)\,\mathrm{d}t. \end{aligned} \tag{13b}$$

Although the left-hand side of (13a) is regular in the lower half-plane $\Im m(\alpha) < \Im m(k)$, the regularity of the right-hand side is violated by the presence of simple poles occurring at the zeros of $K\sin K(b-a)$ lying in the lower half-plane, namely at $\alpha = -\alpha_m$ with α_m being given by

$$\alpha_m = \sqrt{k^2 - \left(\frac{m\pi}{b-a}\right)^2}, \quad m = 0, 1, 2, \ldots. \tag{14}$$

Similarly, the regularity of the right-hand side of (13b) in the upper half-plane $\Im m(\alpha) > \Im m(-k)$ is violated by the presence of simple poles occurring at the zeros of $K\sin Kb$ lying in the upper half-plane, namely

$$\beta_m = \sqrt{k^2 - \left(\frac{m\pi}{b}\right)^2}, \quad m = 0, 1, 2, \ldots. \tag{15}$$

The above-mentioned pole singularities at $\alpha = -\alpha_m$ and $\alpha = \beta_m$ can be eliminated by imposing the condition that their residues are zero. This gives

$$\dot{F}_-(-\alpha_m, b) = -\mathrm{i}\alpha_m(-1)^m\frac{b-a}{2}f_m \tag{16a}$$

and

$$\dot{F}_+(\beta_m, b) = (-1)^m\frac{b}{2}[g_m - \mathrm{i}\beta_m h_m], \tag{16b}$$

where K_m, γ_m, f_m, g_m, and h_m stand for:

$$K_m = K(\alpha_m), \tag{16c}$$

$$\gamma_m = K(\beta_m), \tag{16d}$$

$$f_m = \frac{2}{b-a}\int_a^b f(t)\cos K_m(t-a)\,\mathrm{d}t, \tag{16e}$$

$$\begin{bmatrix} g_m \\ h_m \end{bmatrix} = \frac{2}{b}\int_0^b \begin{bmatrix} g(t) \\ h(t) \end{bmatrix}\cos\gamma_m t\,\mathrm{d}t. \tag{16f}$$

Consider now the continuity relations (3g) and (3i) which read in the Fourier transform domain as:

$$F_-(\alpha,b) + \mathrm{e}^{\mathrm{i}\alpha\ell}F_+(\alpha,b) = G_-(\alpha,b) + \mathrm{e}^{\mathrm{i}\alpha\ell}G_+(\alpha,b). \tag{17}$$

Taking into account (6), (11a), (11b) and (17) one obtains

$$\frac{\dot{F}_-(\alpha,b)}{K^2M_1(\alpha)} + \mathrm{e}^{\mathrm{i}\alpha\ell}\frac{\dot{F}_+(\alpha,b)}{K^2M_2(\alpha)} - F_1(\alpha,b) = \frac{\mathrm{i}\alpha}{K\sin K(b-a)}\int_a^b f(t)\cos K(t-a)\,\mathrm{d}t + \frac{\mathrm{e}^{\mathrm{i}\alpha\ell}}{K\sin Kb}\int_0^b [g(t) - \mathrm{i}\alpha h(t)]\cos Kt\,\mathrm{d}t \tag{18a}$$

with

$$M_1(\alpha) = \frac{\sin K(b-a)}{K}\mathrm{e}^{\mathrm{i}K(b-a)} \tag{18b}$$

and

$$M_2(\alpha) = \frac{\sin Kb}{K}\mathrm{e}^{\mathrm{i}Kb}. \tag{18c}$$

As to the functions $f(t), g(t)$, and $h(t)$, owing to (16e) and (16f), they can be expanded into cosine series as follows:

$$f(t) = \sum_{m=0}^{\infty}\frac{f_m}{p_m}\cos K_m(t-a), \tag{19a}$$

$$\begin{bmatrix} g(t) \\ h(t) \end{bmatrix} = \sum_{m=0}^{\infty}\frac{1}{p_m}\begin{bmatrix} g_m \\ h_m \end{bmatrix}\cos\gamma_m t. \tag{19b}$$

Here we put

$$p_m = \begin{cases} 2, & m = 0, \\ 1, & m \neq 0. \end{cases} \tag{19c}$$

Substituting (19a)–(19c) in (18a) and evaluating the resultant integral, one obtains the following Modified Wiener–Hopf Equation of the third kind valid in the strip $\Im m(-k) < \Im m(\alpha) < \Im m(k)$:

$$\frac{\dot{F}_{-}(\alpha, b)}{K^2 M_1(\alpha)} + \mathrm{e}^{\mathrm{i}\alpha\ell} \frac{\dot{F}_{+}(\alpha, b)}{K^2 M_2(\alpha)} - F_1(\alpha, b) = \mathrm{i}\alpha \sum_{m=0}^{\infty} \frac{f_m}{p_m} \frac{(-1)^m}{K^2 - K_m^2} + \mathrm{e}^{\mathrm{i}\alpha\ell} \sum_{m=0}^{\infty} \frac{[g_m - \mathrm{i}\alpha h_m]}{p_m} \frac{(-1)^m}{K^2 - \gamma_m^2}. \tag{20}$$

A formal solution of (20) can easily be obtained through the classical Wiener–Hopf procedure. The result is:

$$\begin{aligned} \frac{\dot{F}_{-}(\alpha, b)}{(k-\alpha) M_1^{-}(\alpha)} = &- \sqrt{\frac{2k}{\pi\ell}} \mathrm{e}^{-\mathrm{i}\pi/4} \mathrm{e}^{\mathrm{i}kl} \frac{\mathscr{F}[\ell(k-\alpha)]}{k-\alpha} M_1^{+}(k) \dot{F}_{+}(k, b) \\ &- \sum_{m=0}^{\infty} \frac{f_m}{p_m} \frac{\mathrm{i}(-1)^m (k+\alpha_m) M_1^{+}(\alpha_m)}{2(\alpha - \alpha_m)}, \end{aligned} \tag{21a}$$

$$\begin{aligned} \frac{\dot{F}_{+}(\alpha, b)}{(k+\alpha) M_2^{+}(\alpha)} = &- \sqrt{\frac{2k}{\pi\ell}} \mathrm{e}^{-\mathrm{i}\pi/4} \mathrm{e}^{\mathrm{i}kl} \frac{\mathscr{F}[\ell(k+\alpha)]}{k+\alpha} M_2^{+}(k) \dot{F}_{-}(-k, b) \\ &+ \sum_{m=0}^{\infty} \frac{[g_m + \mathrm{i}\beta_m h_m]}{p_m} \frac{(-1)^m (k+\beta_m) M_1^{+}(\beta_m)}{2\beta_m(\alpha + \beta_m)}. \end{aligned} \tag{21b}$$

Here, $M_1^{+}(\alpha)$ and $M_2^{+}(\alpha)$ are the split functions, regular and free of zeros in the upper half-plane $\Im m(\alpha) > \Im m(-k)$, resulting from the Wiener–Hopf factorization of the functions $M_1(\alpha)$ and $M_2(\alpha)$ as:

$$M_1(\alpha) = M_1^{+}(\alpha) M_1^{-}(\alpha), \tag{22a}$$
$$M_2(\alpha) = M_2^{+}(\alpha) M_2^{-}(\alpha), \tag{22b}$$

while $\mathscr{F}(z)$ stands for the modified Fresnel integral defined by

$$\mathscr{F}(z) = -2\mathrm{i}\sqrt{z}\mathrm{e}^{-\mathrm{i}z} \int_z^{\infty} \mathrm{e}^{\mathrm{i}t^2} \, \mathrm{d}t. \tag{23}$$

The explicit expressions of $M_1^{\pm}(\alpha)$ and $M_2^{\pm}(\alpha)$ can be obtained by following the procedure outlined in [10]:

$$\begin{aligned} M_1^{+}(\alpha) = &\sqrt{\frac{\sin k(b-a)}{k}} \exp\left\{ \frac{\mathrm{i}(b-a)K}{\pi} \ln\left(\frac{\alpha+K}{k}\right) \right\} \\ &\times \exp\left\{ \frac{\mathrm{i}(b-a)\alpha}{\pi} \left(1 - \mathscr{C} + \ln\left(\frac{2\pi}{k(b-a)}\right) + \mathrm{i}\frac{\pi}{2}\right) \right\} \\ &\times \prod_{m=1}^{\infty} \left(1 + \frac{\alpha}{\alpha_m}\right) \exp\left[\frac{\mathrm{i}\alpha(b-a)}{m\pi}\right], \end{aligned} \tag{24}$$

where $\mathscr{C}$ is Euler's constant given by $\mathscr{C} = 0.57721\ldots$

$M_2^{+}(\alpha)$ can be found from (24) by replacing $(b-a)$ by b and α_m by β_m.

2.3. Determination of the constants $\mathrm{f_m}, \mathrm{g_m}$ and $\mathrm{h_m}$

Consider now the waveguide region $y \in (0,a),\ x<0$ where the scattered field $u_3(x,y)$ can be expanded into a series of normal modes as follows:

$$u_3(x,y) = \sum_{n=0}^{\infty} \frac{a_n}{p_n} \mathrm{e}^{-\mathrm{i}\zeta_n x} \cos Z_n y \tag{25}$$

with $\zeta_n = \sqrt{k^2 - ((n\pi)/a)^2}$ and $Z_n = K(\zeta_n)$. Similarly, in the waveguide region $y \in (0,b),\ x \in (0,\ell)$, we will express the scattered field $u_4(x,y)$ in terms of normal modes:

$$u_4(x,y) = \sum_{n=0}^{\infty} \frac{[b_n \mathrm{e}^{\mathrm{i}\beta_n x} + c_n \mathrm{e}^{-\mathrm{i}\beta_n x}]}{p_n} \cos \gamma_n y. \tag{26}$$

Note that the solutions of the Wiener–Hopf equation in (21a) and (21b) involve three sets of unknown constants f_m, g_m, and h_m. In order to determine these constants, consider finally the continuity relations (3k)–(3n) with (10c)–(10e). From these relations we have:

$$\frac{\partial}{\partial x} u_4(0,y) = \begin{cases} \frac{\partial}{\partial x} u_3(0,y) + \frac{\partial}{\partial x} u^{\mathrm{i}}(0,y), & y \in (0,a), \\ 0, & y \in (a,b), \end{cases} \tag{27a}$$

$$u_4(0,y) = u_3(0,y) + u^{\mathrm{i}}(0,y), \quad y \in (0,a), \tag{27b}$$

$$\frac{\partial}{\partial x} u_4(\ell,y) = g(y), \quad y \in (0,b), \tag{27c}$$

$$u_4(\ell,y) = h(y), \quad y \in (0,b). \tag{27d}$$

Using (25), (26), (19a), and (19b) in (27a)–(27d), one obtains:

$$\sum_{n=0}^{\infty} \mathrm{i}\beta_n \frac{[b_n - c_n]}{p_n} \cos \gamma_n y = \begin{cases} -\sum_{m=0}^{\infty} \mathrm{i}\zeta_m \frac{a_m}{p_m} \cos Z_m y + \mathrm{i}k, & y \in (0,a), \\ 0, & y \in (a,b), \end{cases} \tag{28a}$$

$$\sum_{n=0}^{\infty} \frac{[b_n + c_n]}{p_n} \cos \gamma_n y = \sum_{m=0}^{\infty} \frac{a_m}{p_m} \cos Z_m y + 1, \quad y \in (0,a), \tag{28b}$$

$$\sum_{n=0}^{\infty} \mathrm{i}\beta_n \frac{[b_n \mathrm{e}^{\mathrm{i}\beta_n \ell} - c_n \mathrm{e}^{-\mathrm{i}\beta_n \ell}]}{p_n} \cos \gamma_n y = \sum_{n=0}^{\infty} \frac{g_n}{p_n} \cos \gamma_n y, \quad y \in (0,b), \tag{28c}$$

$$\sum_{n=0}^{\infty} \frac{[b_n \mathrm{e}^{\mathrm{i}\beta_n \ell} + c_n \mathrm{e}^{-\mathrm{i}\beta_n \ell}]}{p_n} \cos \gamma_n y = \sum_{n=0}^{\infty} \frac{h_n}{p_n} \cos \gamma_n y, \quad y \in (0,b). \tag{28d}$$

Now let us multiply both sides of (28a), (28c) and (28d) by $\cos \gamma_n y,\ n = 0,1,2,\ldots,$ and integrate from $y=0$ to $y=b$. Similarly, multiply both sides of (28b) by $\cos Z_m y,\ m = 0,1,2,\ldots,$ and integrate from $y=0$ to $y=a$. After straight-forward computations we obtain:

$$\frac{b}{a}\frac{b_0-c_0}{2}=-\frac{a_0}{2}+1, \tag{29a}$$

$$\frac{b}{2}\beta_n(b_n-c_n)=-\sum_{m=0}^{\infty}\frac{\zeta_m}{p_m}a_m I_{nm}+\frac{\sin\gamma_n a}{\gamma_n}, \tag{29b}$$

$$a\left(1+\frac{a_0}{2}\right)=\frac{a}{2}(b_0+c_0)+\sum_{n=1}^{\infty}(b_n+c_n)\frac{\sin\gamma_n a}{\gamma_n}, \tag{29c}$$

and

$$\frac{a}{2}a_m=\sum_{n=1}^{\infty}(b_n+c_n)I_{nm}, \tag{29d}$$

where

$$I_{nm}=\begin{cases}\frac{\gamma_n(-1)^m}{\gamma_n^2-Z_m^2}\sin\gamma_n a, & \gamma_n\neq Z_m,\\ a/2, & \gamma_n=Z_m,\end{cases} \tag{29e}$$

and

$$2\mathrm{e}^{\mathrm{i}\beta_n\ell}b_n=g_n+\mathrm{i}\beta_n h_n, \tag{29f}$$

$$-2\mathrm{e}^{-\mathrm{i}\beta_n\ell}c_n=g_n-\mathrm{i}\beta_n h_n. \tag{29g}$$

By eliminating a_m between (29a)–(29d), one gets:

$$\left(1+\frac{b}{a}\right)b_0+\left(1-\frac{b}{a}\right)c_0+\frac{2}{a}\sum_{n=1}^{\infty}(b_n+c_n)\frac{\sin\gamma_n a}{\gamma_n}=4, \tag{30a}$$

$$\frac{bk}{a}\frac{\sin\gamma_n a}{\gamma_n}\frac{(b_0-c_0)}{2}-\frac{b}{2}\beta_n(b_n-c_n)-\frac{2}{a}\sum_{m=1}^{\infty}(b_m+c_m)\sum_{r=1}^{\infty}\zeta_r I_{nr}I_{mr}=0,\quad m=1,2,3\ldots \tag{30b}$$

On the other hand, by substituting $\alpha=\alpha_n$ in (21a) and (21b) and using (16a), (16b) and (29a), (29b), one gets the following results:

$$\frac{b-a}{2}\frac{\alpha_n(-1)^n f_n}{(k+\alpha_n)M_1^+(\alpha_n)}-\sqrt{\frac{2k}{\pi\ell}}\mathrm{e}^{\mathrm{i}\pi/4}\frac{\mathscr{F}[\ell(k+\alpha_n)]}{k+\alpha_n}M_1^+(k)bc_0$$
$$+\sum_{m=0}^{\infty}\frac{f_m}{p_m}\frac{(-1)^m(k+\alpha_m)M_1^+(\alpha_m)}{2(\alpha_n+\alpha_m)}=0,\quad n=0,1,2,3,\ldots, \tag{31a}$$

$$\frac{b\,\mathrm{e}^{-\mathrm{i}\beta_n\ell}(-1)^n c_n}{(k+\beta_n)M_2^+(\beta_n)}+\sqrt{\frac{2k}{\pi\ell}}\mathrm{e}^{\mathrm{i}\pi/4}\mathrm{e}^{\mathrm{i}kl}\frac{\mathscr{F}[\ell(k+\beta_n)]}{k+\beta_n}M_2^+(k)k\frac{b-a}{2}f_0$$
$$+\sum_{m=0}^{\infty}\frac{\mathrm{e}^{\mathrm{i}\beta_m\ell}b_m}{p_m}\frac{(-1)^m(k+\beta_m)M_1^+(\beta_m)}{\beta_m(\beta_n+\beta_m)}=0,\quad n=0,1,2,3,\ldots \tag{31b}$$

The unknown constants b_n, c_n, and f_n can now be determined by solving (31a) and (31b) together with (30a) and (30b). These infinite system of linear algebraic equations are solved approximately by truncating the expansion series. In the numerical results the truncation number N of n is taken as $N = 10$.

3. Radiated field

In this section the radiated field in the region $y > b$ and the aperture field at $x = \ell, y \in (0, b)$ will be considered. The radiated field can be obtained by taking the inverse Fourier transform of $F(\alpha, y)$. By using (8) we write

$$u_1(x,y) = \frac{1}{2\pi}\int_{\mathscr{L}} \frac{\dot{F}_-(\alpha,b) + e^{i\alpha\ell}\dot{F}_+(\alpha,b)}{iK(\alpha)} e^{iK(\alpha)(y-b)} e^{-i\alpha x}\, d\alpha, \tag{32}$$

where $\mathscr{L}$ is a straight line parallel to the real axis lying in the strip $\Im m(-k) < \Im m(\alpha) < \Im m(k)$. The asymptotic evaluation of the integral in (32) through the saddle-point technique yields the far-field expression as follows:

$$u_1(x,y) = -\frac{e^{i\pi/4}}{\sqrt{2\pi}}\left[\dot{F}_-(-k\cos\phi_1, b)\frac{e^{ik\rho_1}}{\sqrt{k\rho_1}} + \dot{F}_+(-k\cos\phi_2, b)\frac{e^{ik\rho_2}}{\sqrt{k\rho_2}}\right], \tag{33a}$$

where (ρ_1, ϕ_1) and (ρ_2, ϕ_2) refer to the cylindrical polar coordinates defined by (see Fig. 2):

$$x = \rho_1\cos\phi_1, \quad y - b = \rho_1\sin\phi_1, \tag{33b}$$

$$x - \ell = \rho_2\cos\phi_2, \quad y - b = \rho_2\sin\phi_2. \tag{33c}$$

As to the aperture field, it can be computed from the infinite series in (26) by putting $x = \ell$:

$$u_4(\ell,y) = \sum_{n=0}^{\infty} \frac{[b_n e^{i\beta_n\ell} + c_n e^{-i\beta_n\ell}]}{p_n}\cos\gamma_n y, \quad y \in (0,b). \tag{34}$$

In order to show the effectiveness as well as the accuracy of the method, the final expressions (33a) and (34) are computed numerically for some particular values of the parameters a, b, ℓ, etc.

Fig. 3 shows the variation of the amplitude of the normalized far-field with the observation angle ϕ_1 for the case $a = b$. The Wiener–Hopf solution of the box-like horn radiator obtained in this paper agrees very well with the already known results related to the parallel plate waveguide [10], as expected.

Fig. 4 shows the far-field patterns of the finite structure depicted in Fig. 5 and the data corresponding to the infinite feed waveguide. In the case of the finite configuration, the results were already obtained by means of a technique developed in [6]. As it is seen, the agreement among both sets of graphs is satisfactory.

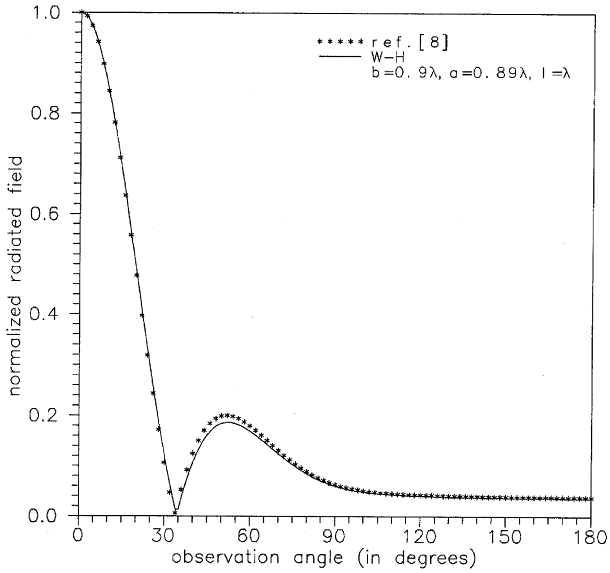

Fig. 3. Comparison with open-ended parallel plate waveguide results.

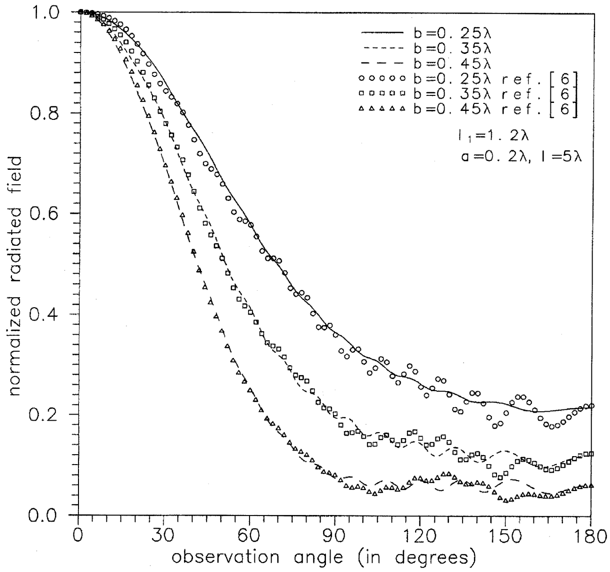

Fig. 4. Normalized radiated field versus the observation angle for different values of b.

Fig. 6 depicts the normalized radiated field versus the observation angle for different values of ℓ.

Figs. 7 and 8 show the variation of the amplitude of the aperture fields for different values of a and ℓ, respectively, when b is fixed. It is seen that although the aperture field increases with increasing values of a, it remains relatively insensitive to the variation of ℓ.

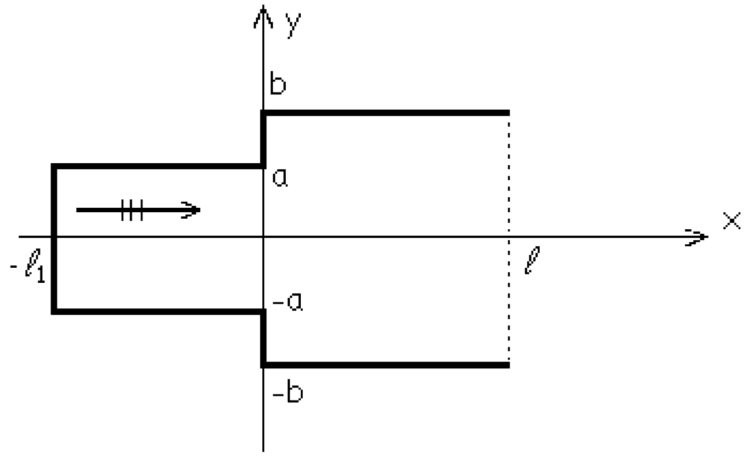

Fig. 5. Two-dimensional finite box-like horn radiator.

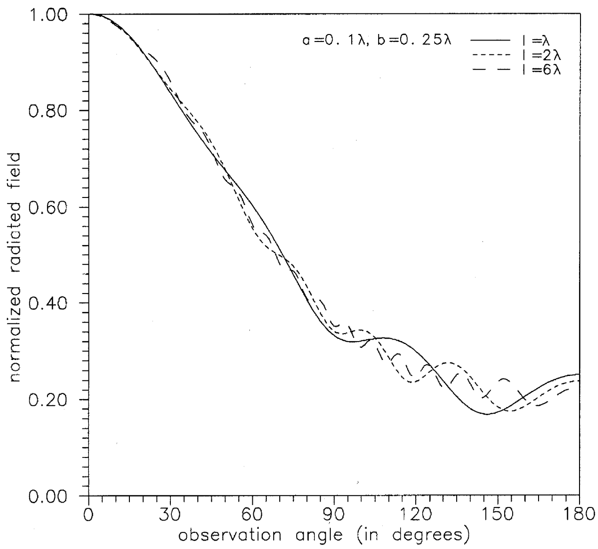

Fig. 6. The normalized field versus the observation angle for different values of ℓ.

4. Concluding remarks

In this work a rigorous Wiener–Hopf analysis is carried out to obtain the radiation characteristics of a box-like horn antenna. Some numerical results are presented to show the effects of various parameters on the radiation phenomenon. The results are compared with those obtained by applying the method developed in [6,7] where the waveguide is assumed to be finite and found very satisfactory. This comparison shows that our results can be used as a benchmark solution for testing some numerical techniques devoted to analyze some finite-length waveguide structures.

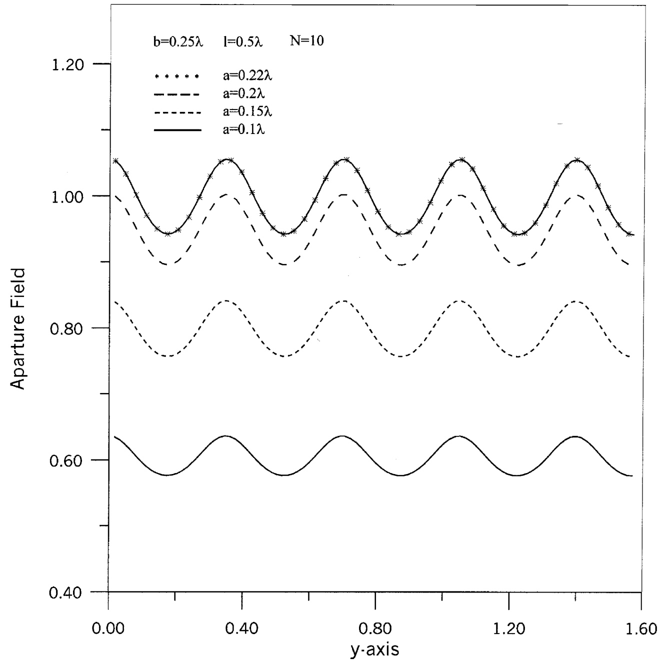

Fig. 7. The variation of the amplitude of the aperture field with respect to y, for different values of a.

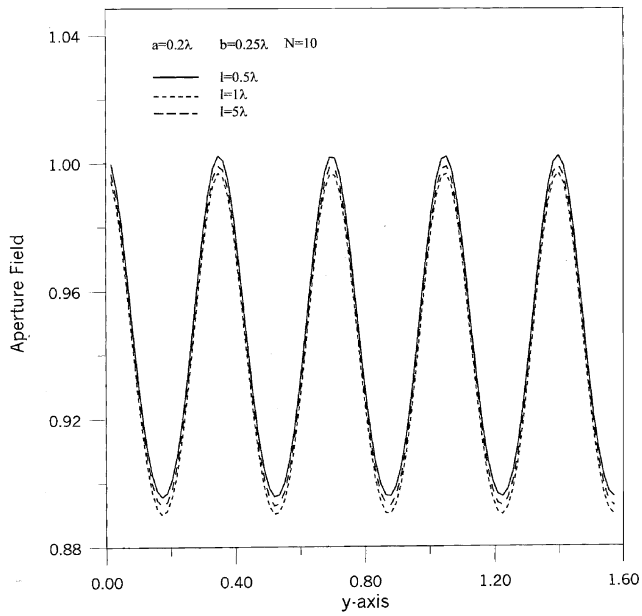

Fig. 8. The variation of the amplitude of the aperture field with respect to y, for different values of ℓ.

The essential advantage of the method adopted in this paper over the other techniques is that it can be applied for a broad range of frequency and can easily be generalized to impedance boundary case. Although the numerical techniques are limited with the sizes of the radiating structure, no such restriction is required in the Wiener–Hopf analysis.

References

[1] J.S. Yu, R.C. Rudduck, L. Peters Jr., Comprehensive analysis for E-plane patterns of horn antennas by edge diffraction theory, IEEE Trans. Antennas Propag. AP-14 (1966) 138–149.

[2] J.S. Yu, R.C. Rudduck, H-plane patterns of a pyramidal horn, IEEE Trans. Antennas Propag. AP-17 (1969) 651–652.

[3] C.A. Mentzer, L. Peters Jr., R.C. Rudduck, Slope diffraction and its application to horns, IEEE Trans. Antennas Propag. AP-23 (1975) 153–159.

[4] M.S. Narasiman, K.S. Rao, GTD analysis of the near field patterns of pyramidal horns, Proc. IEE 126 (1979) 1223–1226.

[5] R.C. Menendez, S.W. Lee, On the role of geometrical optics field in aperture diffraction, IEEE Trans. Antennas Propag. AP-23 (1977) 187–193.

[6] V.P. P'yankov, V.P. Chumachenko, Solution of H-plane radiation problem for two dimensional horn with complex piecewise linear contour, Izv VUZ Radiofiz. 33 (1990) 604–610 (in Russian).

[7] V.P. P'yankov, Electrodynamic characteristics of the box-like horn, Radiotech. Electron. 38 (1993) 2014–2017 (in Russian).

[8] A. Büyükaksoy, B. Polat, Plane wave diffraction by a thick walled parallel plate waveguide, IEEE Trans. Antennas Propag. AP-46 (11) (1998) 1692–1699.

[9] A. Büyükaksoy, F. Birbir, Analysis of an impedance loaded parallel-plate waveguide radiator, J. Electromagn. Waves Appl. 12 (1998) 1509–1526.

[10] B. Noble, Methods Based on the Wiener–Hopf Technique, Chelsea, New York, 1988.